
















SEARCH FOR SHAPE COEXISTENCE IN  
Ca ISOTOPES BY  $(n_{\text{th}}, \gamma)$  REACTIONS\*

M. LUCIANI <sup>a,b</sup>, S. BOTTONI <sup>a,b</sup>, N. CIEPLICKA-ORYŃCZAK <sup>d</sup>  
S. LEONI <sup>a,b</sup>, B. FORNAL <sup>d</sup>, C. MICHELAGNOLI <sup>c</sup>, Ł. ISKRA <sup>d</sup>  
M. JENTSCHEL <sup>c</sup>, U. KÖSTER <sup>c</sup>, N. MĂRGINEAN <sup>e</sup>  
R. MĂRGINEAN <sup>e</sup>, C. MIHAI <sup>e</sup>, P. MUTTI <sup>c</sup>  
S. PASCU <sup>e</sup>, C.A. UR <sup>f</sup>

<sup>a</sup>Università degli Studi di Milano, Milano, Italy

<sup>b</sup>INFN Sezione di Milano, Milano, Italy

<sup>c</sup>ILL, Grenoble, France

<sup>d</sup>Institut of Nuclear Physics PAN, Kraków, Poland

<sup>e</sup>IFIN-HH, Bucharest, Romania

<sup>f</sup>ELI-NP, Bucharest, Romania

*Received 16 November 2025, accepted 19 January 2026,  
published online 31 March 2026*

The  $A \sim 40$  mass region is ideal to study the evolution of nuclear structure and to probe different theoretical approaches. In particular, in these nuclei, phenomena like shape coexistence are expected to appear. The objective of this work is to study the evolution of such phenomena across the Ca isotopic chain by performing complete low-spin spectroscopy of even–even  $^{42,44}\text{Ca}$  and odd–even  $^{43,45}\text{Ca}$  isotopes and, together with the already published results on  $^{41,47,49}\text{Ca}$ , track the evolution of nuclear structure along  $Z = 20$ . All four isotopes relevant to this work were populated by  $(n_{\text{th}}, \gamma)$  neutron-capture reactions exploiting thermal neutrons from the ILL (Grenoble) nuclear reactor. In this article, we present preliminary results on  $^{42}\text{Ca}$  and  $^{44}\text{Ca}$ . In our experiments, we used the FIPPS spectrometer to detect  $\gamma$ -rays, and both double- $\gamma$ - and triple- $\gamma$ -coincidence techniques were used to reconstruct the decay schemes. The result is 10 new levels and 109 new transitions for  $^{42}\text{Ca}$ , and 27 new levels and 280 new  $\gamma$  rays in  $^{44}\text{Ca}$ . Preliminary angular correlation studies of  $^{42}\text{Ca}$  excited states will also be presented, and the population of  $0^+$  excited states, possibly associated with shape coexistence, will be discussed.

DOI:10.5506/APhysPolBSupp.19.1-A17

---

\* Presented at the XXXVIII Mazurian Lakes Conference on Physics, Piaski, Poland, August 31–September 6, 2025.

## 1. Introduction

Shape coexistence refers to the appearance of distinct shapes of the same nucleus at low excitation energy in a narrow energy range [1–4]. This is a very well-known phenomenon nowadays that has been deeply studied in heavy systems (*e.g.*, in Pb nuclei [5]), although similar phenomena were observed in several other regions of the nuclear chart systems (*e.g.*, in the lighter systems of Cd, Zr, and Ni [6–8]).

In this context, along with theoretical predictions, experimental data provide valuable information which helps to shed light on the microscopic nature of shape coexistence driven by nucleon correlations. For this reason, the  $Z = 20$  isotopic chain is an ideal testing ground because different theoretical methods can be used to tackle different nuclear spectroscopic properties. Here, the predictive power of large-scale shell model calculations and Density Functional Theory can be tested and compared even with *ab-initio* calculations, which can now be applied in these medium-mass regions [9–11]. Moreover, evidence of shape coexistence has already been found in  $^{42}\text{Ca}$  and  $^{44}\text{Ca}$ . Hadyńska-Klek *et al.* [12, 13] demonstrated the presence of a super-deformed slightly-triaxial band lying over the  $0_1^+$  state of  $^{42}\text{Ca}$  at 1837 keV with a  $6p-4h$  character, as suggested by their Gogny D1S calculations, which confirmed the original description of the microscopic character of this state given by Fortune *et al.* [14], who described it as resulting from the admixture of  $4p-2h$  and  $6p-4h$  excitations. Moreover, Fortune and collaborators [15] described the first excited  $0_1^+$  state of  $^{44}\text{Ca}$  at 1883 keV as resulting from the admixture of  $4p$  and  $6p-2h$  excitations. In this contribution, we will focus on the study of  $^{42}\text{Ca}$  and  $^{44}\text{Ca}$ . Together with already published results on  $^{41,47,49}\text{Ca}$  by our collaboration [16], the new results will allow us to further investigate the evolution of the structure of semi-magic Ca isotopes in between the  $N = 20$  and  $N = 28$  neutron shell closures, when going towards the neutron-rich side of the nuclear chart along  $Z = 20$ .

## 2. The experimental setup

Two neutron capture experiments were conducted at the Institut Laue-Langevin nuclear reactor facility (ILL) [17], aiming to populate and study  $^{42}\text{Ca}$  and  $^{44}\text{Ca}$  with the neutron capture reactions  $^X\text{Ca}(n, \gamma)^{X+1}\text{Ca}$ . The ILL reactor is currently the most intense continuous neutron source for research purposes in the world, with a neutron flux of  $\sim 10^8 \text{ n cm}^{-2} \text{ s}^{-1}$  at the end of the FIPPS beam line.

The FISSION Product Prompt  $\gamma$ -ray Spectrometer (FIPPS) [18], shown in Fig. 1, was used for  $\gamma$ -ray detection. It is a  $\gamma$ -ray spectrometer composed of 8 HPGe clover detectors, each clover containing 4 HPGe crystals for a total of 32 detectors placed on a circular frame around the scattering chamber. Each clover is equipped with a set of BGO scintillators for Compton suppression.

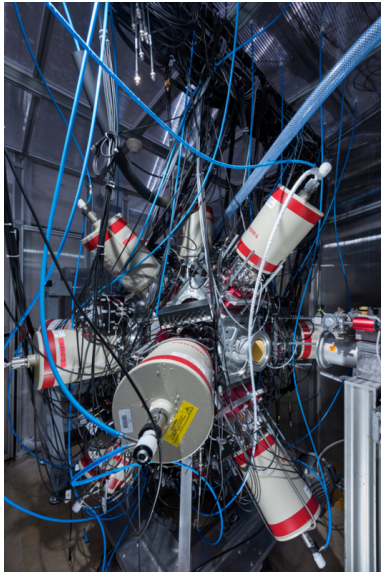


Fig. 1. The FIPPS (Fission Product Prompt  $\gamma$ -ray Spectrometer) at ILL, in its 16 (FIPPS+IFIN) clover detectors configuration [18].

Other than in its stand-alone arrangement, FIPPS is designed to be used in two other configurations:

- FIPPS+16 LaBr<sub>3</sub>:Ce detectors for lifetime measurements,
- FIPPS+8 clover HPGe detectors (IFIN) to enhance geometrical efficiency.

The former was used for the  $^{42}\text{Ca}$  experiment and the latter for the  $^{44}\text{Ca}$  one.

During the experiments, two powdered Ca targets were used:

- $^{41}\text{Ca}$  (radioactive) 600  $\mu\text{g}$ , 2 MBq,  $\tau_{1/2} \approx 10^5$  y,
- $^{43}\text{Ca}$  (stable) 20 mg.

It is the first time that these nuclei have been investigated with neutron-capture reactions employing a high-resolution composite  $\gamma$ -ray spectrometer. Previous experiments were conducted in the 1970s and 1980s with only a few detectors [19, 20].

### 3. Data analysis

The level scheme and the  $\gamma$ -ray decay paths of  $^{42}\text{Ca}$  and  $^{44}\text{Ca}$  were studied using double- $\gamma$  and triple- $\gamma$  coincidence techniques. As a first step in the analysis, we identified all the  $\gamma$ -ray transitions and levels belonging

to the nuclei of interest by placing coincidence gates on known primary and secondary transitions. With this technique, we were able to identify  $\gamma$  lines coming from target contaminants. Figure 2 shows an example of the effectiveness of this method, highlighting the capability of distinguishing between real  $^{44}\text{Ca}$  transitions and contaminants (*e.g.*,  $^{36}\text{Cl}$ ), in the case of the  $^{43}\text{Ca}(n_{\text{th}},\gamma)$  reaction. Figure 2 top panels show the two coincidence gates (light gray/red shadowed areas) placed on the  $^{44}\text{Ca}$  7773 keV primary transition (a) and on the  $^{36}\text{Cl}$  1164 keV secondary transition (b). In both cases, the background regions are shown by dark gray/blue shadowed areas, respectively. Panels (c)–(d) and (e)–(f) show the projected spectra obtained with the previous gates; here, transitions assigned to the parent nucleus are labelled with their energies.

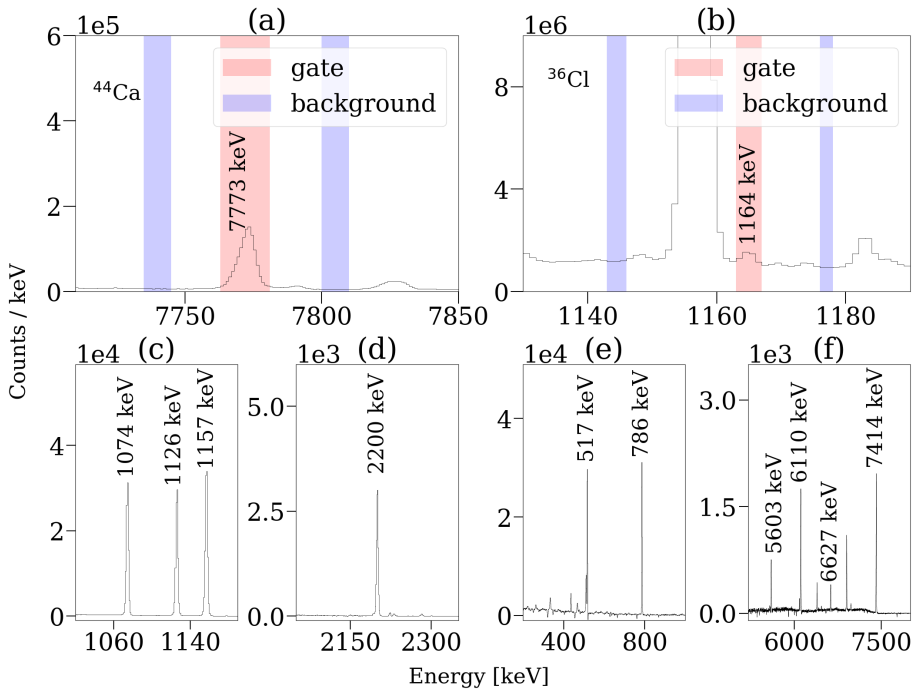


Fig. 2. (Colour on-line) (a)  $\gamma$ -ray spectra where the light gray/red area indicates the coincidence gate placed on the 7773 keV  $^{44}\text{Ca}$  primary transition; dark gray/blue areas indicate the background region used for subtraction. (b) The same as the previous panel, but the coincidence gate is set on the 1164 keV  $^{36}\text{Cl}$  transition. (c)–(d) Projected spectra obtained from the coincidence gate set in panel (a); transitions assigned to  $^{44}\text{Ca}$  are labelled with their energies. (e)–(f) Two energy regions of the spectra obtained from the coincidence gate set in panel (b); transitions assigned to  $^{36}\text{Cl}$  are labelled with their energies. (Data obtained from the  $^{43}\text{Ca}(n_{\text{th}},\gamma)$  reaction.)

The analysis allowed us to expand the already existing level scheme of both  $^{42}\text{Ca}$  and  $^{44}\text{Ca}$  with many new levels and transitions never observed before. Specifically, we added 109 transitions and 10 new levels to the  $^{42}\text{Ca}$  level scheme, and 280 transitions and 27 levels to the  $^{44}\text{Ca}$  level scheme. In the case of  $^{44}\text{Ca}$ , a partial result of this work is presented in Figs. 3 and 4, focusing on the decay from the capture state. In these figures, previously known  $\gamma$  rays and states are shown in black and newly found in gray/red.

Through the use of a multi-detector  $\gamma$ -ray spectrometer like FIPPS,  $\gamma$ -ray angular correlations can be studied. This allows us to determine  $\gamma$ -ray multipolarities and helps to assign spins and parities of new states. This becomes crucial to possibly identify  $0^+$  states. An example of the result obtained with this procedure is plotted in Fig. 5, where the case of the 899 keV  $2_2^+ \rightarrow 2_1^+$  and the 1524 keV  $2_1^+ \rightarrow 0_{\text{GS}}^+$  [E2] transitions of  $^{42}\text{Ca}$  is presented. In particular, Fig. 5 panel (a) shows a schematic representation of the decay path involving the two transitions of interest. Panel (b) shows a portion of the coincidence matrix zoomed over the coincidence peak between the 899 keV and the 1524 keV transitions (top), the experimental angular correlation points, the experimental fitted curve and the angular correlation curve reported by the literature (bottom). Following this analysis, there was no evidence of new  $0^+$  states in the excitation scheme of  $^{42}\text{Ca}$  populated during our neutron-capture experiment. A possible explanation could be due to the  $3^-/4^-$  spin-parity of the neutron-capture state, which does not allow for a direct decay to  $0^+$  state. The same approach will be used to investigate the  $0^+$  population in  $^{44}\text{Ca}$ , where a high density of states was found and  $0^+$  states might be populated in subsequent decays.

As the last part of this work, the neutron capture energy of  $^{42}\text{Ca}$  was evaluated by considering all the possible decay paths from the capture state  $S_n$  to the ground state, obtaining a value of  $S_n = 11479.5(16)$  keV. This value is found to be compatible with the  $S_n = 11480.67(6)$  keV value reported in the literature. The same approach will also be followed in the analysis of  $^{44}\text{Ca}$ .

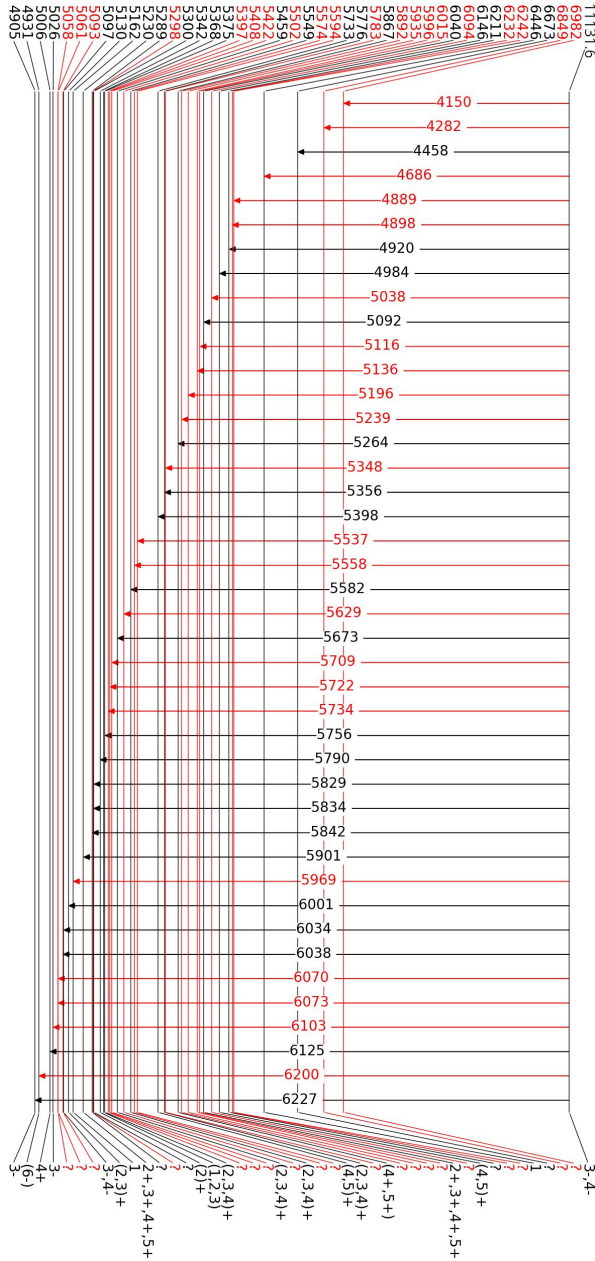


Fig. 3. (Colour on-line)  $^{44}\text{Ca}$  partial decay scheme showing only primary  $\gamma$  rays from the  $^{43}\text{Ca}(n_{\text{th}}, \gamma)$  reaction. Black lines represent levels and transitions known before this work. Gray/red lines represent newly found levels and transitions. Unknown spin-parities are marked with a question mark.



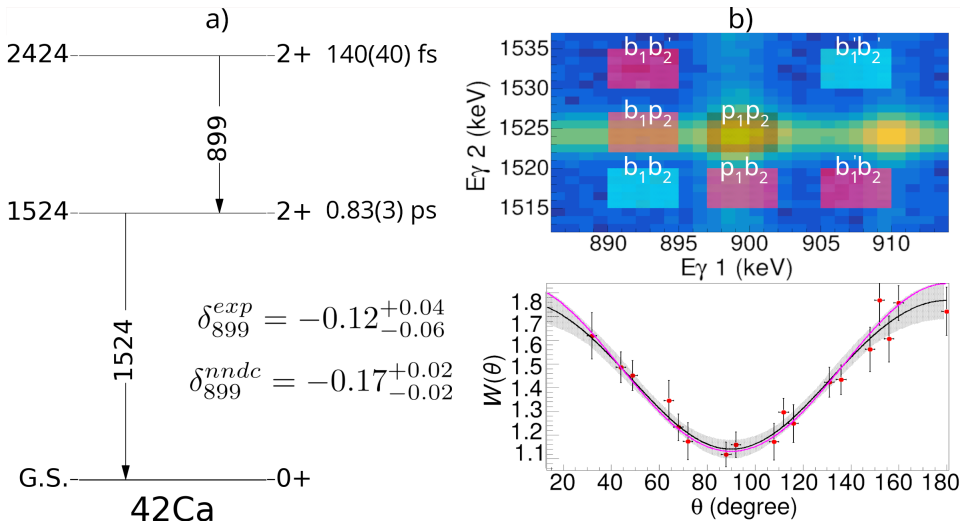


Fig. 5. (Colour on-line) (a)  $^{42}\text{Ca}$  partial level scheme showing the two transitions of interest for this example (*i.e.*, the 899 keV  $2_2^+ \rightarrow 2_1^+$  and the 1524 keV  $2_1^+ \rightarrow 0_{\text{GS}}^+$  [E2]). (b) Top: Portion of the  $\gamma$ - $\gamma$  matrix showing the corresponding coincidence peak. The central gate ( $p_1 p_2$ ) defines the peak region, while light-blue ( $b_1 b_2$  and  $b'_1 b'_2$ ) and red ( $b_1 p_2$ ,  $p_1 b_2$ ,  $b'_1 b'_2$ , and  $b_1 b'_2$ ) gates define regions of background and spurious coincidences. The net counts in the coincidence peak are then evaluated as the difference between the counts in the peak region and those obtained by combining the light-blue and red background regions defined before, as described in [21]. Bottom: Experimental angular correlation points (red dots), fitted angular distribution (black solid line and grey error bar, giving the mixing ratio value  $\delta_{899}^{\text{exp}} = -0.12^{+0.04}_{-0.06}$ ) and angular correlation curve obtained imposing the mixing ratio  $\delta_{899}^{\text{nndc}} = -0.17$  reported on Nuclear Data Center Website [22] (gray/pink line).

#### 4. Conclusions

Two neutron capture experiments were performed at the Institut Laue-Langevin to investigate the structure of Ca isotopes using the FIPPS spectrometer. The results on  $^{42}\text{Ca}$  and  $^{44}\text{Ca}$  allowed us to substantially expand their level and  $\gamma$ -decay schemes through the use of  $\gamma$ - $\gamma$  and  $\gamma$ - $\gamma$ - $\gamma$  coincidence techniques. Angular correlations between  $\gamma$  rays were successfully tested on known transitions of  $^{42}\text{Ca}$  and were used to characterise new  $\gamma$  rays and excited states found in this work. No new  $0^+$  states were found lying between the ground state and the neutron capture energy of  $^{42}\text{Ca}$ . In the future, the same angular correlations analysis will be performed on  $^{44}\text{Ca}$  to pin down the possible presence of  $0^+$  states that could be the fingerprint of shape coexistence.

## REFERENCES

- [1] K. Heyde, J.L. Wood, *Rev. Mod. Phys.* **83**, 1467 (2011).
- [2] P.E. Garrett, M. Zielińska, E. Clément, *Prog. Part. Nucl. Phys.* **124**, 103931 (2022).
- [3] S. Leoni *et al.*, *Prog. Part. Nucl. Phys.* **139**, 104119 (2024).
- [4] S. Leoni, B. Fornal, N. Mărginean, J. Wilson, *Eur. Phys. J. Spec. Top.* **233**, 1061 (2024).
- [5] A.N. Andreyev *et al.*, *Nature* **405**, 430 (2000).
- [6] S. Leoni *et al.*, *Phys. Rev. Lett.* **118**, 162502 (2017).
- [7] N. Mărginean *et al.*, *Phys. Rev. Lett.* **125**, 102502 (2020).
- [8] C. Kremer *et al.*, *Phys. Rev. Lett.* **117**, 172503 (2016).
- [9] J.D. Holt, J. Menéndez, J. Simonis, A. Schwenk, *Phys. Rev. C* **90**, 024312 (2014).
- [10] Y. Utsuno *et al.*, *Prog. Theor. Phys. Suppl.* **196**, 304 (2012).
- [11] M. Bender, P.H. Heenen, P.G. Reinhard, *Rev. Mod. Phys.* **75**, 121 (2003).
- [12] H. Hadyńska-Kleńk *et al.*, *Phys. Rev. Lett.* **117**, 062501 (2016).
- [13] H. Hadyńska-Kleńk *et al.*, *Phys. Rev. C* **97**, 024326 (2018).
- [14] H.T. Fortune *et al.*, *Nucl. Phys. A* **294**, 208 (1978).
- [15] H.T. Fortune *et al.*, *Phys. Lett. B* **79**, 205 (1978).
- [16] S. Bottoni *et al.*, *Phys. Rev. C* **103**, 014320 (2021).
- [17] <https://www.ill.eu/a-unique-facility/the-worlds-most-intense-neutron-source/the-ill-high-flux-reactor>
- [18] <https://ill.eu/users/instruments/instruments-list/fipps/characteristics>
- [19] S.W. Kikstra *et al.*, *Nucl. Phys. A* **496**, 429 (1989).
- [20] D.H. White, R.E. Birkett, *Phys. Rev. C* **5**, 513 (1972).
- [21] <https://past-bite-3c1.notion.site/AngCorr-soft-userguide-c0a7ab73274e4c56ac8d0fcc40aec4bd>
- [22] <https://www.nndc.bnl.gov>